

## On the Soliton Structures of the (2+1)-Dimensional Long Wave-Short Wave Resonance Interaction Equation with Two Analytical Techniques and its Bifurcation Analysis

S M Rayhanul Islam\*

\*Department of Mathematics, Pabna University of Science and Technology, Pabna-6600, Bangladesh.

### ABSTRACT

The (2+1)-dimensional long-wave-short-wave resonance interaction (LWSWRI) equation has extensive applications in various fields of science and engineering. The (2+1)-dimensional LWSWRI equation and two analytical techniques have been considered in this manuscript. These schemes, via the advanced auxiliary equation, improve F-expansion techniques applied to the considered model and obtain soliton solutions with a lot of parameters. These derived soliton solutions manifest as trigonometric, hyperbolic, rational, and exponential function solutions, highlighting their utility as mathematical tools. The study offers visual representations, including both three-dimensional (3D) and two-dimensional (2D) combined charts, to illustrate selected solutions and demonstrate the influence of parameters. Furthermore, the bifurcation analysis (BA) of the model is studied through the planar dynamical systems. The stability of the equilibrium points (EPs) and a graphical representation of the phase chart of the system are investigated. The Hamiltonian function is also derived in this manuscript. These methodologies function as dependable, straightforward, and powerful instruments for examining diverse nonlinear evolution equations encountered in physics, applied mathematics, engineering, and other disciplines.

© 2024 Published by Bangladesh Mathematical Society

**Received:** March 13, 2024    **Accepted:** April 23, 2024    **Published Online:** June 30, 2024

**Keywords:** the (2+1)-dimensional LWSWRI equation; AAE scheme; IFE scheme; Bifurcation analysis; Nonlinear model.

**AMS Subject Classifications 2024:** 35C05, 35C07, 35C08, 35C99

### 1. Introduction

Nowadays, the exploration of nonlinear wave phenomena has emerged as a pivotal area of research worldwide. Nonlinear wave models offer a valuable framework for analysing these complex phenomena. Consequently, numerous researchers have dedicated their efforts to studying these models, aiming for precise wave solutions and an understanding of nonlinear wave phenomena. Its significance extends beyond theoretical realms to real-life applications across diverse fields including shallow water wave propagation [1], mathematical fluid dynamics [2], nonlinear optics [3], plasma physics [4], nano-biosciences [5], finance [6], optical fiber [7], communication systems [8], and numerous other domains.

In the last three decades, a multitude of researchers have delved into NLMs in pursuit of numerous analytic solutions. This quest for solutions holds significant importance as it aids in unravelling the

\*Corresponding author. E-mail address: rayhanulmath@yahoo.com, rayhanul\_math@pust.ac.bd

underlying dynamics and physical properties of nonlinear wave phenomena. By extracting solutions from NLMs, researchers gain valuable insights into the intricate workings of these phenomena. For example, Kamrujjaman et al. [9] have delved into the intricate dynamics of phenomena by leveraging solutions from NLMs. Their study explores the competitive reaction-diffusion model, focusing on the emergence of traveling wave solutions for two competing species. Additionally, they investigate the influence of competitive-cooperative coefficients. Furthermore, Kamrujjaman et al. [10] analyse the Burgers equation using the tan-cot function method, examining both its inviscid and viscous versions in the context of fluid flow. Their investigation includes an exploration of the effects of internal friction on fluid dynamics, elucidated through the Reynolds number. Consequently, investigators have successfully employed a diverse array of analytical and numerical approaches to find solutions for NLMs. Notable among these approaches are the generalized Kudryashov [11], the Riccati sub-equation [12], the advanced auxiliary equation (AAE) [13, 14], the extended hyperbolic function [15], the  $(G'/G, 1/G)$ -expansion [16], the improved F-expansion (IFE) [17, 18], the unified [19], the enhanced modified simple equation [20], the extended  $(G'/G^2)$ -expansion [21], the Nucci's reduction [22], the new extended generalized Kudryashov [23], the improved modified extended tanh-function [24], Hirota's bilinear [25], Darboux transformation [26], and several other methodologies. These powerful and effective schemes are constantly being refined and are specifically designed to build soliton solutions for NLMs. They are skilfully made to extract new solutions for the NLMs, whose solutions are of great importance to physics, fluid mechanics, and many other scientific and technical domains.

In the realm of mathematical physics, numerous researchers have explored nonlinear mathematical models (NLMs) to uncover soliton solutions, particularly for analysing wave phenomena in fluid dynamics. Examples include the Korteweg-de Vries equation, the Burgers equation, the Benjamin-Ono equation, and the (2+1)-dimensional dispersive long wave equation in shallow water [27]. It's well established that a significant interaction between long and short waves emerges when the phase velocity of the long wave closely aligns with the component of the short wave's group velocity in the direction of the long wave's propagation. This phenomenon can be viewed as a distinct manifestation of the three-wave resonant interaction [28]. In 1976, Yajima and Oikawa [29] demonstrated that the NLMs governing this interaction are amenable to exact solutions through the inverse scattering method and yielding  $N$ -soliton solutions, which are bright-type solitons. Ma and Redekopp [30] reformulated the equations into Hirota's bilinear forms [31], and yielding soliton solutions wherein the short wave appears as a uniform plane wave at infinity, which is alongside the bright-type  $N$ -soliton solution. At the same time, Benny [32] explored the resonance between long and short waves in two-dimensional wave propagation, focusing on capillary-gravity waves in deep water. Unlike in shallow water, obtaining simple interaction equations proved challenging due to the absence of long wave behaviours in deep water conditions. Conversely, Grimshaw [33] derived straightforward interaction equations elucidating the resonant interplay between long and short internal waves propagating obliquely in a stably stratified fluid. However, the discussion did not extend to their solutions. In 1983, Funakoshi and Oikawa [34] conducted a comprehensive numerical investigation into the initial value problems associated with these equations, and they also extended the interaction equations for the resonance between a long internal wave and a short surface wave in a two-layer fluid to the case in which they propagate obliquely each other and discussed some solutions to the extended interaction equations. In 1989, Oikawa et al. [35] expanded the concept of long-short resonance to (2+1)-dimensional scenarios, integrating the propagation of oblique waves. The resulting (2+1)-dimensional LWSWRI equation is represented as:

$$i(u_t + u_y) - u_{xx} + uv = 0, \quad (1.1)$$

$$v_t - 2(|u|^2)_x = 0, \quad (1.2)$$

In the context of the (2+1)-dimensional LSWRI equation, this interaction manifests as a nonlinear coupling between the long wave field  $u$  and the short-wave field  $v$ . In Eqs. (1.1) and (1.2), the short surface wave packets represent as  $u = u(x, y, t)$ , the long interfacial wave represents as  $v = v(x, y, t)$ , the term  $uv$  represents the nonlinear interaction between the long and short-wave fields. This interaction can lead to various effects, such as the modulation of wave amplitudes, the generation of new wave frequencies through wave mixing, the formation of solitons or other coherent structures, and the transfer of energy between different wave modes.

From my observations, numerous researchers have delved into the (2+1)-dimensional LSWRI model, exploring soliton solutions through various techniques. Additionally, the introduction of an arbitrary function of the seed solutions has unveiled a wealth of coherent soliton structures within this model. In a specific instance, authors employed the variable separation approach to derive exact solutions to the (2+1)-dimensional LSWRI equation [36]. Yan [37] has investigated new Jacobi elliptic function solutions to the considered model through the sinh-Gordon expansion method. Radha et al. [38] have investigated the (2+1)-dimensional LSWRI equation by using the Painleve truncation approach, and they generated a wide class of elliptic function periodic wave solutions. Xin et al. [39] have studied the existence and uniqueness of the global smooth solution to the (2+1)-dimensional LSWRI equation. Kumar and Chand [40] have inspected the soliton solution to the system of Eqs. (1.1) and (1.2) through the projective Riccati equation method. In Mirzazadeh [41], the modified simple equation method has been used to construct exact periodic and soliton solutions of the (2+1)-dimensional LSWRI equation. Kanna et al. [42] have obtained mixed soliton solutions of the (2+1)-dimensional multi-component long-wave-short-wave resonance interaction system by applying Hirota's bilinearization method. Khare et al. [43] have explored exact periodic solutions to the (2+1)-dimensional LSWRI equation by using the Lamé function ansatz. Chen et al. [44] have derived a bright-dark multi-soliton solution to the (2+1)-dimensional multi-component LSWRI system with the help of KP hierarchy reduction. Cimpoiasu and Pauna [45] have explored the exact solutions of the LSWRI system through the trial equation and the generalized Kudryashov methods. Jia and Zuo have studied the long-wave-short-wave resonance interaction through the bilinear method and attained soliton solutions [46]. The soliton solutions obtained from these studies hold potential applications in the science and engineering fields.

Upon examining prior research conducted by multiple scholars, it becomes evident that there has been no exploration of soliton solutions for the (2+1)-dimensional LSWRI equation employing both AAE and IFE techniques (both methods are detailed in Appendices A and B). Furthermore, there is a notable void in the literature, as prior authors have not conducted bifurcation analysis or shown the way to stable solutions for the wave variable. Our paper introduces these methods and performs a thorough analysis of the model to close this gap.

This study has two goals in mind: First, we will obtain soliton solutions of the (2+1)-dimensional LSWRI equation using AAE and IFE approaches and analyse the effect of parameters. We will also offer physical and graphical representations of some of the solutions that fit inside the model's structure. Second, in order to investigate the possibility of other solutions, we will apply planar dynamical theory to the BA of the model.

The format of the paper is as follows: The techniques used to investigate soliton solutions of the (2+1)-dimensional LSWRI equation in Section 2 and the comparison between our solutions and Mirzazadeh [41] solutions are shown in the same section. In Section 3, the impact of parameters is discussed, and the graphical and physical explanations of certain solutions are discussed. The BA of the considered model is analyzed in Section 4. Section 5 provides a thorough summary of our

results in conclusion.

## 2. Mathematical Conduct of the Model

In this segment, we will smear the AAE and IFE schemes on the (2+1)-dimensional LWSWRI equation to explore the soliton solutions, and the mathematical analysis is given below:

To complex wave transformation [39]

$$u(x, t) = U(\xi)e^{i\delta}, v(x, t) = \wp(\xi), \xi = x + (\omega - 2\alpha)y + \omega t, \delta = \alpha x + \beta y + \tau t$$

in Eqs. (1.1) and (1.2), we get the real part as

$$U''(\xi) + (\beta + \tau - \alpha^2)U(\xi) - U(\xi)\wp(\xi) = 0, \tag{2.1}$$

and imaginary parts as

$$\omega\wp'(\xi) - 2(U^2(\xi))' = 0. \tag{2.2}$$

Integrating Eq. (2.2) with respect to  $\xi$  and taking the integration constant as zero yields

$$\wp(\xi) = \frac{2}{\omega}U^2(\xi). \tag{2.3}$$

Substituting Eq. (2.3) into Eq. (2.1), yields

$$U''(\xi) + (\beta + \tau - \alpha^2)U(\xi) - \frac{2}{\omega}U^3(\xi) = 0, \tag{2.4}$$

where  $\alpha, \beta, \tau$  and  $\omega$  are real constant.

### 2.1. The AAE scheme applied to the stated model

By using the balancing procedure in (2.4), yields  $N = 1$ , The general solution takes the form

$$U(\xi) = c_0 + c_1d^{f(\xi)}. \tag{2.5}$$

In Eq. (2.5),  $c_0$  and  $c_1$  are constants with  $c_1 \neq 0$  and the function  $f(\xi)$  satisfies the first order auxiliary equation  $f'(\xi) = \frac{1}{\ln(d)}\{\lambda d^{-f(\xi)} + \mu + \sigma d^{f(\xi)}\}$ . Substituting Eq. (2.5) into Eq. (2.4), we derive algebraic equations, which upon solving, the following solution sets yields:

$$\omega = \frac{4c_0^2}{\mu^2}, \tau = \alpha^2 - 2\lambda\sigma + \frac{\mu^2}{2}, c_0 = c_0, c_1 = \frac{2c_0\sigma}{\mu}, \tag{2.6}$$

Using Eqs. (2.6) and (2.5) with regards to the solutions of the auxiliary equation, the solutions of the (2+1)-dimensional LWSWRI equation as follows:

When  $\mu^2 - 4\lambda\sigma < 0$  and  $\sigma \neq 0$ ,

$$u_1(x, y, t) = \frac{c_0\sqrt{4\lambda\sigma - \mu^2}}{\mu} \tan\left(\frac{\sqrt{4\lambda\sigma - \mu^2}}{2}(x + (\omega - 2\alpha)y + \omega t)\right) e^{i(\alpha x + \beta y + \tau t)},$$

and

$$u_2(x, y, t) = -\frac{c_0\sqrt{4\lambda\sigma - \mu^2}}{\mu} \cot\left(\frac{\sqrt{4\lambda\sigma - \mu^2}}{2}(x + (\omega - 2\alpha)y + \omega t)\right) e^{i(\alpha x + \beta y + \tau t)},$$

When  $\mu^2 - 4\lambda\sigma > 0$  and  $\sigma \neq 0$ ,

$$u_3(x, y, t) = -\frac{c_0\sqrt{\mu^2 - 4\lambda\sigma}}{\mu} \tanh\left(\frac{\sqrt{\mu^2 - 4\lambda\sigma}}{2}(x + (\omega - 2\alpha)y + \omega t)\right) e^{i(\alpha x + \beta y + \tau t)},$$

and

$$u_4(x, y, t) = -\frac{c_0\sqrt{\mu^2 - 4\lambda\sigma}}{\mu} \coth\left(\frac{\sqrt{\mu^2 - 4\lambda\sigma}}{2}(x + (\omega - 2\alpha)y + \omega t)\right) e^{i(\alpha x + \beta y + \tau t)},$$

When  $\mu^2 + 4\lambda^2 < 0, \sigma \neq 0$  and  $\sigma = -\lambda$ ,

$$u_5(x, y, t) = \frac{c_0\sqrt{-\mu^2 - 4\lambda^2}}{\mu} \tan\left(\frac{\sqrt{-\mu^2 - 4\lambda^2}}{2}(x + (\omega - 2\alpha)y + \omega t)\right) e^{i(\alpha x + \beta y + \tau t)},$$

and

$$u_6(x, y, t) = -\frac{c_0\sqrt{-\mu^2-4\lambda^2}}{\mu} \cot\left(\frac{\sqrt{-\mu^2-4\lambda^2}}{2}(x + (\omega - 2\alpha)y + \omega t)\right) e^{i(ax+\beta y+\tau t)},$$

When  $\mu^2 + 4\lambda^2 > 0, \sigma \neq 0$  and  $\sigma = -\lambda$ ,

$$u_7(x, y, t) = -\frac{c_0\sqrt{\mu^2+4\lambda^2}}{\mu} \tanh\left(\frac{\sqrt{\mu^2+4\lambda^2}}{2}(x + (\omega - 2\alpha)y + \omega t)\right) e^{i(ax+\beta y+\tau t)},$$

and

$$u_8(x, y, t) = -\frac{c_0\sqrt{\mu^2+4\lambda^2}}{\mu} \coth\left(\frac{\sqrt{\mu^2+4\lambda^2}}{2}(x + (\omega - 2\alpha)y + \omega t)\right) e^{i(ax+\beta y+\tau t)},$$

When  $\mu^2 - 4\lambda^2 < 0$  and  $\sigma = \lambda$ ,

$$u_9(x, y, t) = \frac{c_0\sqrt{4\lambda^2-\mu^2}}{\mu} \tan\left(\frac{\sqrt{4\lambda^2-\mu^2}}{2}(x + (\omega - 2\alpha)y + \omega t)\right) e^{i(ax+\beta y+\tau t)},$$

and

$$u_{10}(x, y, t) = -\frac{c_0\sqrt{4\lambda^2-\mu^2}}{\mu} \cot\left(\frac{\sqrt{4\lambda^2-\mu^2}}{2}(x + (\omega - 2\alpha)y + \omega t)\right) e^{i(ax+\beta y+\tau t)},$$

When  $\mu^2 - 4\lambda^2 > 0$  and  $\sigma = \lambda$ ,

$$u_{11}(x, y, t) = -\frac{c_0\sqrt{\mu^2-4\lambda^2}}{\mu} \tanh\left(\frac{\sqrt{\mu^2-4\lambda^2}}{2}(x + (\omega - 2\alpha)y + \omega t)\right) e^{i(ax+\beta y+\tau t)},$$

and

$$u_{12}(x, y, t) = -\frac{c_0\sqrt{\mu^2-4\lambda^2}}{\mu} \coth\left(\frac{\sqrt{\mu^2-4\lambda^2}}{2}(x + (\omega - 2\alpha)y + \omega t)\right) e^{i(ax+\beta y+\tau t)},$$

When  $\mu^2 = 4\lambda\sigma$ ,

$$u_{13}(x, y, t) = -\frac{c_0}{\sqrt{\sigma\lambda}} \left((x + (\omega - 2\alpha)y + \omega t)\right)^{-1} e^{i(ax+\beta y+\tau t)},$$

When  $\sigma = \mu = K$  and  $\lambda = 0$ ,

$$u_{14}(x, y, t) = -\frac{c_0(e^{K(x+(\omega-2\alpha)y+\omega t)}+1)}{e^{K(x+(\omega-2\alpha)y+\omega t)}-1} e^{i(ax+\beta y+\tau t)},$$

When  $\mu = (\lambda + \sigma)$ ,

$$u_{15}(x, y, t) = \frac{c_0(\sigma-\lambda)(\sigma e^{(\lambda-\sigma)(x+(\omega-2\alpha)y+\omega t)}+1)}{(\lambda+\sigma)(\sigma e^{(\lambda-\sigma)(x+(\omega-2\alpha)y+\omega t)}-1)} e^{i(ax+\beta y+\tau t)},$$

When  $\mu = -(\lambda + \sigma)$ ,

$$u_{16}(x, y, t) = \frac{c_0(\sigma-\lambda)(e^{(\lambda-\sigma)(x+(\omega-2\alpha)y+\omega t)}+\sigma)}{(\lambda+\sigma)(\sigma-e^{(\lambda-\sigma)(x+(\omega-2\alpha)y+\omega t)})} e^{i(ax+\beta y+\tau t)},$$

When  $\lambda = 0$ ,

$$u_{17}(x, y, t) = -\frac{c_0(\sigma e^{\mu(x+(\omega-2\alpha)y+\omega t)}+1)}{(\sigma e^{\mu(x+(\omega-2\alpha)y+\omega t)}-1)} e^{i(ax+\beta y+\tau t)},$$

When  $\sigma = \mu = \lambda \neq 0$ ,

$$u_{18}(x, t) = c_0\sqrt{3} \times \tan\left(\frac{\sqrt{3}\lambda}{2}(x + (\omega - 2\alpha)y + \omega t)\right) e^{i(ax+\beta y+\tau t)},$$

Where  $\omega = \frac{4c_0^2}{\mu^2}$  and  $\tau = \alpha^2 - 2\lambda\sigma + \frac{\mu^2}{2}$ . Under specific conditions, including  $\lambda = \sigma = 0, \mu = \sigma = K$  and  $\lambda = 0$ , and  $\sigma = 0$ , when the constants are replaced, constant solutions are found. However, these solutions are not provided here as they hold no physical significance. Conversely, utilizing the mentioned method, a solution for Eq. (1.1) does not emerge, when  $\lambda\sigma < 0, \mu = 0$  and  $\sigma \neq 0, \mu = 0$  and  $= -\sigma, \lambda = \mu = 0, \sigma = \lambda$  and  $\mu = 0$ , and  $\sigma = \mu = 0$ .

## 2.2. The IFE scheme applied to the stated model

By using the balancing procedure in (2.4), yields  $N = 1$ , the general solution take the form

$$U(\xi) = \alpha_0 + \alpha_1(m + \varphi(\xi)) + \beta_1(m + \varphi(\xi))^{-1}, \tag{2.7}$$

where  $\alpha_0, \alpha_1$  and  $\beta_1$  are constants and to be evaluated latter and  $\alpha_1$  or  $\beta_1$  may be zero, but both  $\alpha_1$  and  $\beta_1$  could not be zero simultaneously. The function  $\varphi(\xi)$  satisfies the first order auxiliary equation  $\varphi'(\xi) = \kappa + \varphi^2(\xi)$ . By substituting Eq. (2.7) into Eq. (2.4) and consolidating all terms, and then setting each coefficient to zero, we derive a system of algebraic equations. Employing Maple software to solve these equations and yields in the resulting solutions set:

Group one:  $\tau = \alpha^2 - \beta - 2\kappa, \alpha_0 = \pm\sqrt{\omega}m, \alpha_1 = \pm\sqrt{\omega}, \beta_1 = 0,$  (2.8)

Group two:  $\tau = \alpha^2 - \beta - 2\kappa, \alpha_0 = \pm\sqrt{\omega}m, \alpha_1 = 0, \beta_1 = \pm(m^2 + \kappa)\sqrt{\omega},$  (2.9)

By employing Eqs. (2.8) and (2.7) alongside the solution of the auxiliary equation, we derive the following solutions for the (2+1)-dimensional LWSWRI equation:

When  $\kappa < 0$ ,

$$u_{19,20}(x, y, t) = \pm\sqrt{\omega} \times \sqrt{-\kappa} \tanh\left(\sqrt{-\kappa}(x + (\omega - 2\alpha)y + \omega t)\right) e^{i(ax+\beta y+\tau t)},$$

and

$$u_{21,22}(x, y, t) = \pm\sqrt{\omega} \times \sqrt{-\kappa} \coth\left(\sqrt{-\kappa}(x + (\omega - 2\alpha)y + \omega t)\right) e^{i(ax+\beta y+\tau t)},$$

When  $\kappa > 0$ ,

$$u_{23,24}(x, y, t) = \pm\sqrt{\omega} \times \sqrt{\kappa} \tan\left(\sqrt{\kappa}(x + (\omega - 2\alpha)y + \omega t)\right) e^{i(ax+\beta y+\tau t)},$$

and

$$u_{25,26}(x, y, t) = \pm\sqrt{\omega} \times \sqrt{\kappa} \cot\left(\sqrt{\kappa}(x + (\omega - 2\alpha)y + \omega t)\right) e^{i(ax+\beta y+\tau t)},$$

When  $\kappa = 0$ ,

$$p_{27,28}(x, y, t) = \pm \frac{\sqrt{\omega} e^{i\left(\frac{\Gamma(1+Y)}{\alpha}(ax^\alpha+bt^\alpha)\right)}}{x+(\omega-2\alpha)y+\omega t}.$$

By employing Eqs. (2.9) and (2.7) alongside the solution of the auxiliary equation, we derive the following solutions for the (2+1)-dimensional LWSWRI equation:

When  $\kappa < 0$ ,

$$u_{29,30}(x, y, t) = \pm\sqrt{\omega} \times \frac{m\sqrt{-\kappa} \tanh\left(\sqrt{-\kappa}(x+(\omega-2\alpha)y+\omega t)\right)^{-\kappa}}{m-\sqrt{-\kappa} \tanh\left(\sqrt{-\kappa}(x+(\omega-2\alpha)y+\omega t)\right)} e^{i(ax+\beta y+\tau t)},$$

and

$$u_{31,32}(x, y, t) = \pm\sqrt{\omega} \times \frac{m\sqrt{-\kappa} \coth\left(\sqrt{-\kappa}(x+(\omega-2\alpha)y+\omega t)\right)^{+\kappa}}{m-\sqrt{-\kappa} \coth\left(\sqrt{-\kappa}(x+(\omega-2\alpha)y+\omega t)\right)} e^{i(ax+\beta y+\tau t)},$$

When  $\kappa > 0$ ,

$$u_{33,34}(x, y, t) = \pm\sqrt{\omega} \times \frac{m\sqrt{\kappa} \tan\left(\sqrt{\kappa}(x+(\omega-2\alpha)y+\omega t)\right)^{-\kappa}}{m+\sqrt{\kappa} \tan\left(\sqrt{\kappa}(x+(\omega-2\alpha)y+\omega t)\right)} e^{i(ax+\beta y+\tau t)},$$

and

$$u_{35,36}(x, y, t) = \pm\sqrt{\omega} \times \frac{m\sqrt{\kappa} \cot\left(\sqrt{\kappa}(x+(\omega-2\alpha)y+\omega t)\right)^{+\kappa}}{m-\sqrt{\kappa} \cot\left(\sqrt{\kappa}(x+(\omega-2\alpha)y+\omega t)\right)} e^{i(ax+\beta y+\tau t)},$$

When  $\kappa = 0$ ,

$$p_{37,38}(x, y, t) = \pm \frac{\sqrt{\omega}m}{m(x+(\omega-2\alpha)y+\omega t)-1} e^{i\left(\frac{\Gamma(1+Y)}{\alpha}(ax^\alpha+bt^\alpha)\right)}.$$

For all the solutions mentioned above to be valid, it is imperative that the condition  $\omega \neq 0$  is satisfied. Under certain conditions, namely  $\rho < 0$  and  $\sigma = 0$ ;  $\rho > 0$  and  $\sigma = 0$ , when the constants are replaced, it has no solution of the both equations for EHF scheme. After substituting all the obtained solutions into Eq. (2.3), we get the solution  $v(x, y, t)$  but not shown in this manuscript.

### 2.3. Comparison between our solutions and Mirzazadeh [41] solutions

In this manuscript, the AAE and IFE schemes have been applied to the LWSWRI equation and soliton solutions from the previous sub-section. By applying the AAE technique, we found eighteen soliton solutions to the LWSWRI equation, and by employing the IFE technique, we found twenty soliton solutions to the LWSWRI equation. Both techniques have some common solutions but are not shown in Table in the manuscript. Mirzazadeh [41] has inspected the LWSWRI equation through the modified simple equation (MSE) scheme and explored five soliton solutions. It is noteworthy that both methods share a common solution, as illustrated in **Table 1**. Finally, it can be claimed that using the AAE approach instead of Mirzazadeh's MSE method for solving the LWSWRI equation yields a substantially higher number of wave solutions [41]. These solutions are expressed through exponential function solutions, rational function solutions, hyperbolic function solutions, and trigonometric function solutions.

**Table 1: Comparison between our solutions and Mirzazadeh [41] solutions:**

<b>Mirzazadeh [41] solutions</b>	<b>Our solutions</b>
Taking $a = 1, p = 1, q = 1, k = -0.5$ and $u_3(x, y, t) = \Phi(x, y, t)$ , then the solution of Eq. (88) turns to $\Phi(x, y, t) = 0.5 \tan\left(\frac{x+y+t}{2}\right) e^{i(x+y-\frac{t}{2})}.$	Taking $c_0 = 1, \mu = 2, \omega = 1, \alpha = 1, \beta = 1, \tau = -0.5, \sigma = 1, \lambda = \frac{5}{4}$ and $u_1(x, y, t) = \Phi(x, y, t)$ , then the solution turns to $\Phi(x, y, t) = 0.5 \tan\left(\frac{x+y+t}{2}\right) e^{i(x+y-\frac{t}{2})}.$
Picking $a = 1, p = 1, q = 1, k = -0.5$ and $u_4(x, y, t) = \Phi(x, y, t)$ , then the solution of Eq. (89) turns to $\Phi(x, y, t) = 0.5 \cot\left(\frac{x+y+t}{2}\right) e^{i(x+y-\frac{t}{2})}.$	Picking $c_0 = -1, \mu = 2, \omega = 1, \alpha = 1, \beta = 1, \tau = -0.5, \sigma = 1, \lambda = \frac{5}{4}$ and $u_2(x, y, t) = \Phi(x, y, t)$ , then the solution turns to $\Phi(x, y, t) = 0.5 \cot\left(\frac{x+y+t}{2}\right) e^{i(x+y-\frac{t}{2})}.$
Taking $a = 1, p = 1, q = 1, k = 5, \mathcal{E} = \sqrt{2.5}$ and $u_5(x, y, t) = \Phi(x, y, t)$ , then the solution of Eq. (90) turns to $\Phi(x, y, t) = \mathcal{E} \tanh(\mathcal{E}(x + y + t)) e^{i(x+y+5t)}.$	Taking $c_0 = -1, \mu = 2, \omega = 1, \alpha = 1, \beta = 1, \mathcal{E} = \sqrt{2}, \tau = 5, \lambda = 1$ and $u_7(x, y, t) = \Phi(x, y, t)$ , then the solution turns to $\Phi(x, y, t) = \mathcal{E} \tanh(\mathcal{E}(x - y + t)) e^{i(x+y+5t)}.$
Taking $a = 1, p = 1, q = 1, k = 5, \mathcal{E} = \sqrt{2.5}$ and $u_5(x, y, t) = \Phi(x, y, t)$ , then the solution of Eq. (91) turns to $\Phi(x, y, t) = \mathcal{E} \coth(\mathcal{E}(x + y + t)) e^{i(x+y+5t)}.$	Taking $c_0 = -1, \mu = 2, \omega = 1, \alpha = 1, \beta = 1, \mathcal{E} = \sqrt{2}, \tau = 5, \lambda = 1$ and $u_8(x, y, t) = \Phi(x, y, t)$ , then the solution turns to $\Phi(x, y, t) = \mathcal{E} \coth(\mathcal{E}(x - y + t)) e^{i(x+y+5t)}.$

**Remarks:** All the established solutions have been validated and found to be correct by putting them into the stated equation.

### 3. Graphical and physical explanation of some solutions

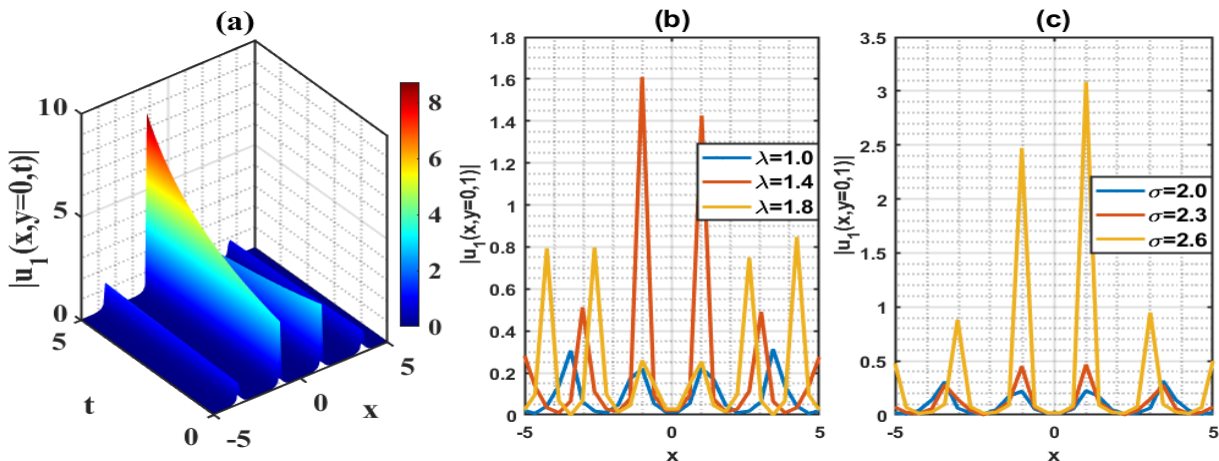
In this segment, we explore the graphical behavior and physical attributes of several solutions obtained using Matlab. These solutions were derived through the effective AAE and IFE methods, encompassing exact soliton solutions, hyperbolic functions, rational solutions, trigonometric functions, and exponential functions. The diversity of functions in these solutions allows us to visualize various graphical structures such as traveling waves, periodic waves, kink waves, and other soliton profiles. Graphs serve as illustrated representations of explicit solutions, facilitating comparison. For dynamic solution analysis, 3D and 2D combined plots of select results are presented in Figures 1, 2, 3, and 4, with appropriate parametric values assigned. A succinct overview of solution dynamics is provided below:

Figure 1 depicts the evolutionary profile dynamics of the solution  $u_1(x, y = 0, t)$  using appropriate parameter values:  $c_0 = 0.02, \lambda = 1, \sigma = 2, \mu = 1, \alpha = 0.3$  and  $\beta = 0.1$ . In the 3D plot (Fig. 1a), a periodic wave profile is illustrated within the interval  $x \in [-5, 5]$  and  $t \in [0, 5]$ . Figures 1(b) and 1(c) exhibit the variation of wave amplitude and phase component, respectively, for different parameter values of  $\lambda = \{1.0, 1.4, 1.8\}$  and  $\sigma = \{2.0, 2.3, 2.6\}$  via 2D plots, showcasing wave propagation across the spatial range  $x \in [-5, 5]$ .

Figure 2 shows the 3D, and 2D combined plots of the solutions  $u_3(x, y, t)$ . The evolutionary profile of the solution was obtained of the appropriate selection of the arbitrary parameters  $c_0 = 0.4, \lambda = 0.2, \sigma = -0.1, \mu = 1, \alpha = 0.3$  and  $\beta = 0.1$ . In Fig. 2(a), the 3D wave profile represents the kink type wave profiles of the selected solutions within the interval  $x \in [-5, 5]$  and  $t \in [0, 5]$ . The variation of wave amplitude and phase component are recorded in the Figs. 2(b) and (c) for the appropriate choice of the parameters  $\lambda = \{0.2, 0.4, 0.6\}$  and  $\sigma = \{-0.1, -0.5, -0.9\}$  via the 2D plot that shows the wave propagation for  $x \in [-5, 5]$ .

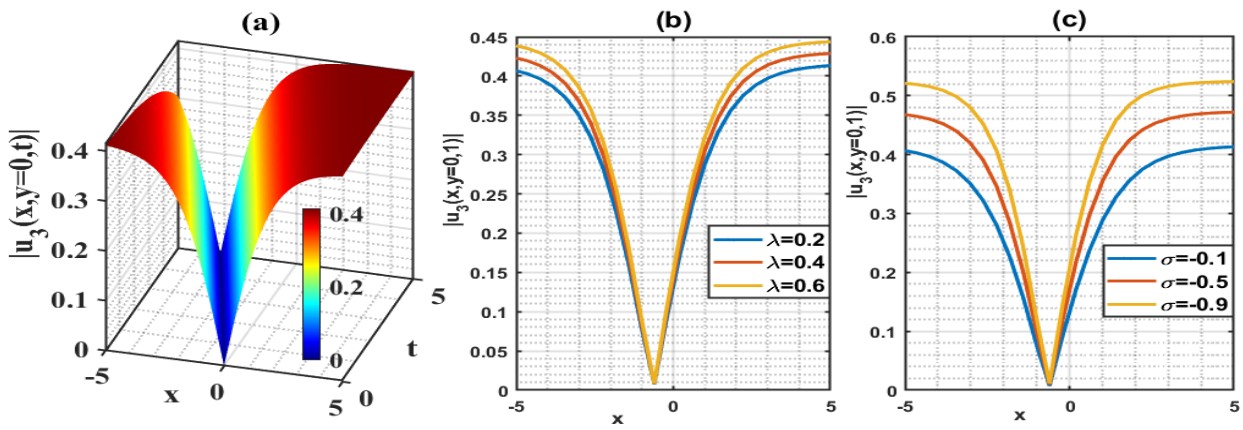
Figure 3 illustrates the graphical view of the solution  $u_{19}(x, y, t)$  for the appropriate values of parameters  $\omega = 1.25, \kappa = -0.09, \alpha = 0.3$  and  $\beta = 0.01$ . Figure 3(a) demonstrates a 3D plot, which represents kink shape wave profile with the range  $x \in [-5, 5]$  and  $t \in [0, 5]$ . Moreover, Figs. 3(b) and (c) illustrates the corresponding 2D representations for the suitable choice of the parameters  $\omega = \{1.0, 1.25, 1.50\}$  and  $\kappa = \{-0.07, -0.09, -0.11\}$ . It is observed that phase component is increase when the value of  $\omega$  increases and  $\kappa$  decreases.

Figure 4 describe the 3D, and 2D combined plots of the obtained solution  $u_{25}(x, y, t)$  for the appropriate values of parameters  $\omega = 0.01, \kappa = 0.52, \alpha = 0.25$  and  $\beta = 1.23$ . In 3D plot, Fig. 4(a) demonstrates the periodic wave profile of the solution  $u_{25}(x, y, t)$  within the interval  $x \in [-5, 5]$  and  $t \in [0, 5]$ . Furthermore, the variation of wave amplitude and phase difference are recorded in Figs. 5(b) and (c) for the appropriate choice of the parameters  $\omega = \{0.01, 0.02, 0.03\}$  and  $\kappa = \{0.52, 0.55, 0.58\}$  via the 2D plot that shows the wave propagation under the range space  $x \in [-5, 5]$ .



**Figure 1:** Dynamics behaviours of the solution  $u_1(x, y, t)$ , (a) Periodic (3D) wave profile (b) Impact of the parameter  $\lambda$ , and (c) Impact of the parameter  $\sigma$ .





**Figure 2:** Dynamics behaviours of the solution  $u_3(x, y, t)$ , (a) Kink (3D) wave profile (b) Impact of the parameter  $\lambda$ , and (c) Impact of the parameter  $\sigma$ .

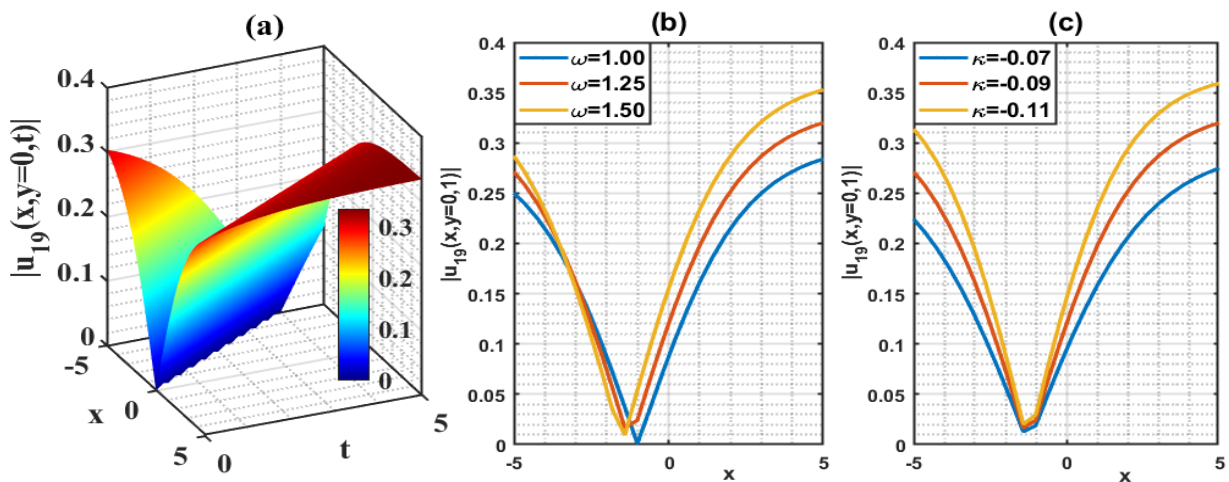


**Figure 3:** Dynamics behaviours of the solution  $u_{19}(x, y, t)$ , (a) Kink (3D) wave profile (b) Impact of the parameter  $\omega$ , and (c) Impact of the parameter  $\kappa$ .

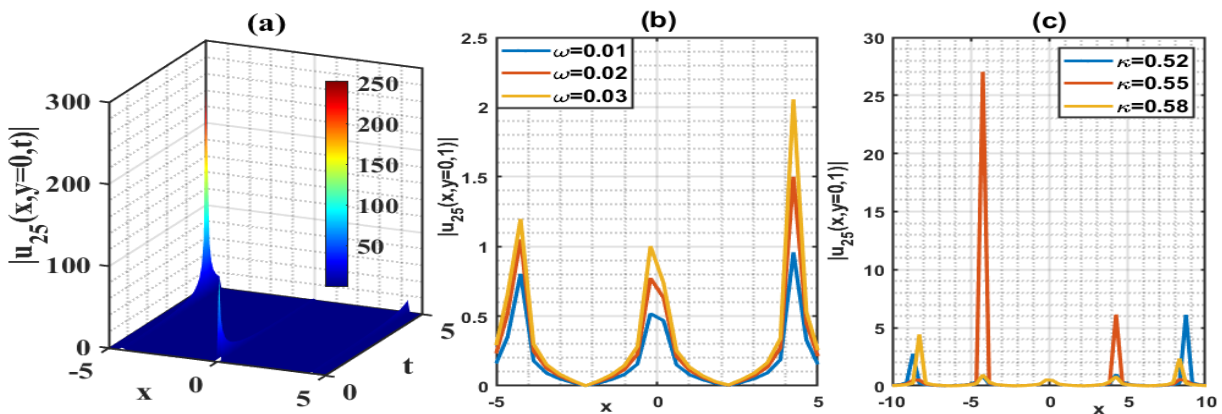


**Figure 4:** Dynamics behaviours of the solution  $u_{25}(x, y, t)$ , (a) Periodic (3D) wave profile (b) Impact of the parameter  $\omega$ , and (c) Impact of the parameter  $\kappa$ .

#### 4. Bifurcation analysis of the model

In this section, we delve into the BA of the specified model using planar dynamical system techniques. By setting  $X = U$  and  $Y = X'$ , we postulate that the system outlined in Eq. (2.4) can be expressed as the following system:

$$\begin{cases} \frac{dX}{d\xi} = Y \\ \frac{dY}{d\xi} = \frac{2}{\omega}X^3 - (\beta + \tau - \alpha^2)X \end{cases} \tag{4.1}$$

In this context, we introduce the well-known phase portraits in the  $(X, Y)$ -plane to depict wave solutions of the considered model.

The system of (4.1) is derived from the associated Hamiltonian function

$$H(X, Y) = \frac{Y^2}{2} - \frac{1}{2\omega}X^4 + \frac{\beta + \tau - \alpha^2}{2}X^2. \tag{4.2}$$

using the Hamilton canonical equations  $X' = \frac{\partial H}{\partial Y}$  and  $Y' = -\frac{\partial H}{\partial X}$ . Currently, the three EPs of equation (4.1) are  $(0, 0)$  and  $\left(\pm\sqrt{\frac{\omega(\beta + \tau - \alpha^2)}{2}}, 0\right)$ , with the condition  $\omega \neq 0$ . The characteristic equation of the Jacobian matrix is expressed as:

$$\Omega^2 - \frac{6}{\omega}X^2 + (\beta + \tau - \alpha^2) = 0.$$

Regarding the EP  $(0, 0)$ , the characteristic roots are  $\pm\sqrt{\Theta}$ , where  $\Theta = \beta + \tau - \alpha^2$ . If  $\Theta > 0$ , the eigenvalues (EV) are real and have opposed signs, rendering the EP an unstable saddle point (USP). Contrariwise, if  $\Theta < 0$ , the EVs are imaginary, indicating that the EP  $(0, 0)$  is a stable center (SC) or ellipse. Through this investigation, it becomes clear that the EP can be categorized as an USP, as depicted in Figs. 5, 7, and 8. On the other hand, the specified point displays an elliptical profile and signifies a SC, as demonstrated in Figs. 5, 6, and 8. Conversely, in terms of the stability of the EPs  $\left(\pm\sqrt{\frac{\omega(\beta + \tau - \alpha^2)}{2}}, 0\right)$ , the characteristic roots are  $\pm\sqrt{\Theta}$ , where  $\Theta = 2(\beta + \tau - \alpha^2)$ . If  $\Theta > 0$ , the EVs are imaginary, indicating a stable center for the given EP. Conversely, if  $\Theta < 0$ , the EVs are real and have opposite signs, classifying the given EPs as USPs. Following this examination, it is apparent that the EPs can be characterized as USPs, as demonstrated in Figs. 5, 7, and 8. Conversely, the stated points exhibit an elliptical profile and represent SC, as depicted in Figs. 5, 6, and 8.

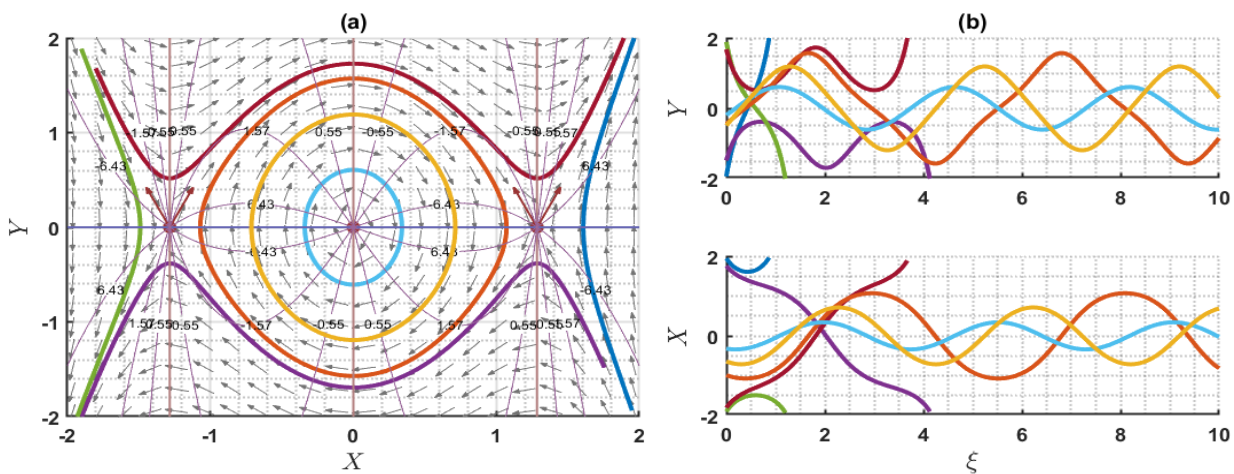
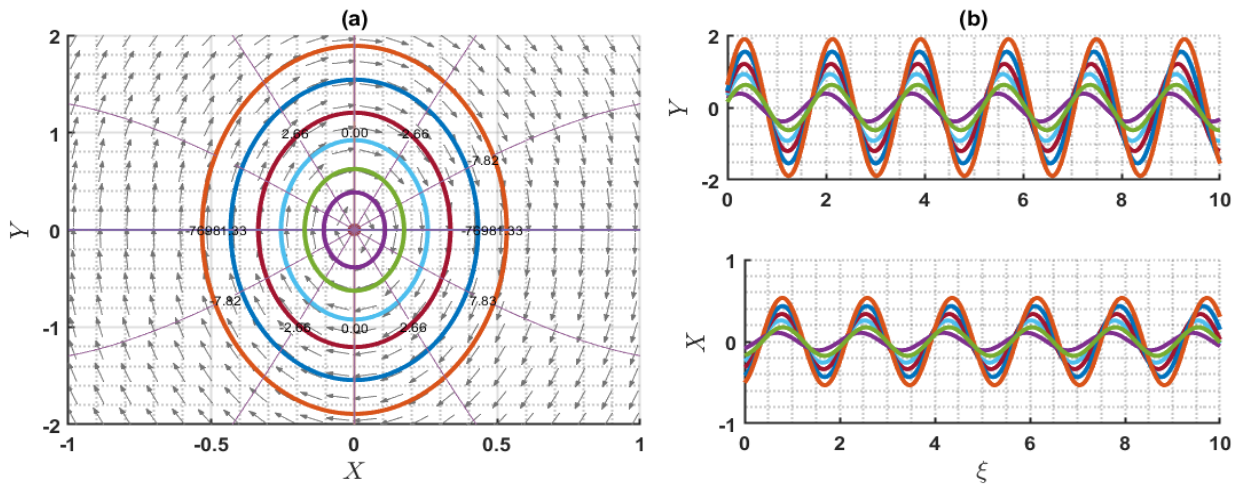
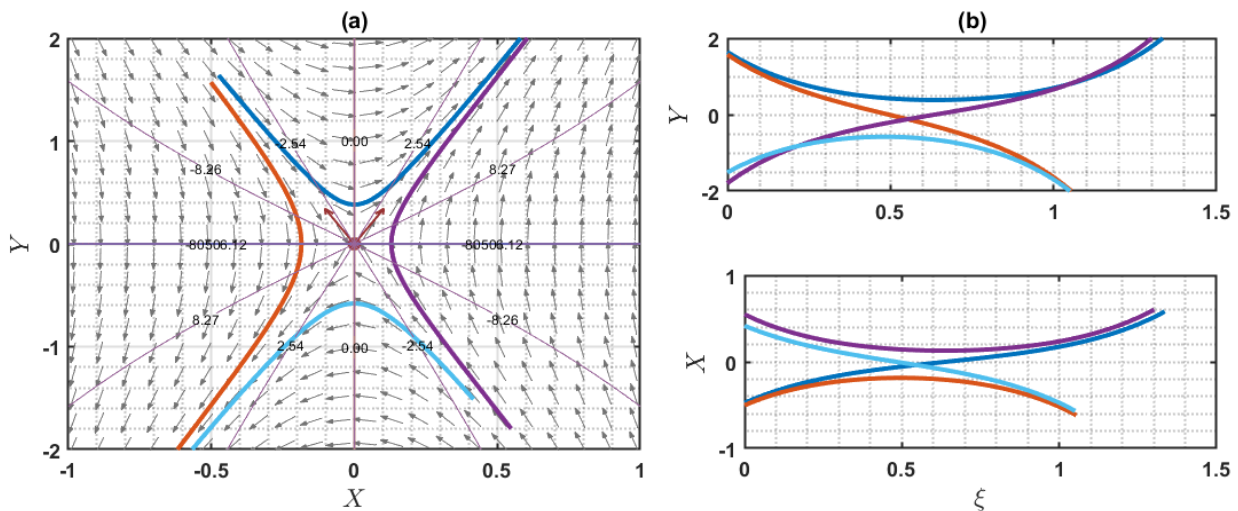


Figure 5: The phase depiction and related solution of the planar dynamical system (4.1) are

existing for designated parameter as  $\omega = 1, \beta = 12, \tau = 0.3, \alpha = 3$ : (a) The possible EP at  $(0,0)$  which is an unstable saddle and the other EP at  $(\pm 1.28, 0)$  are centers, (b) the corresponding solutions of the trajectories in terms of wave variable is depicted.



**Figure 6:** The phase portrait and associated solution of the planar dynamical system (4.1) are presented for selected parameter as  $\omega = 0.7, \beta = 12, \tau = 1, \alpha = 0.1$ : (a) The possible EP at  $(0,0)$  which is center, (b) the corresponding solutions of the trajectories in terms of wave variable is depicted.



**Figure 7:** The phase portrait and associated solution of the planar dynamical system (4.1) are presented for selected parameter as  $\omega = 1, \beta = 10, \tau = 0.5, \alpha = 1.25$ : (a) The possible EP at  $(0,0)$  which is an unstable saddle, (b) the corresponding solutions of the trajectories in terms of wave variable is depicted.

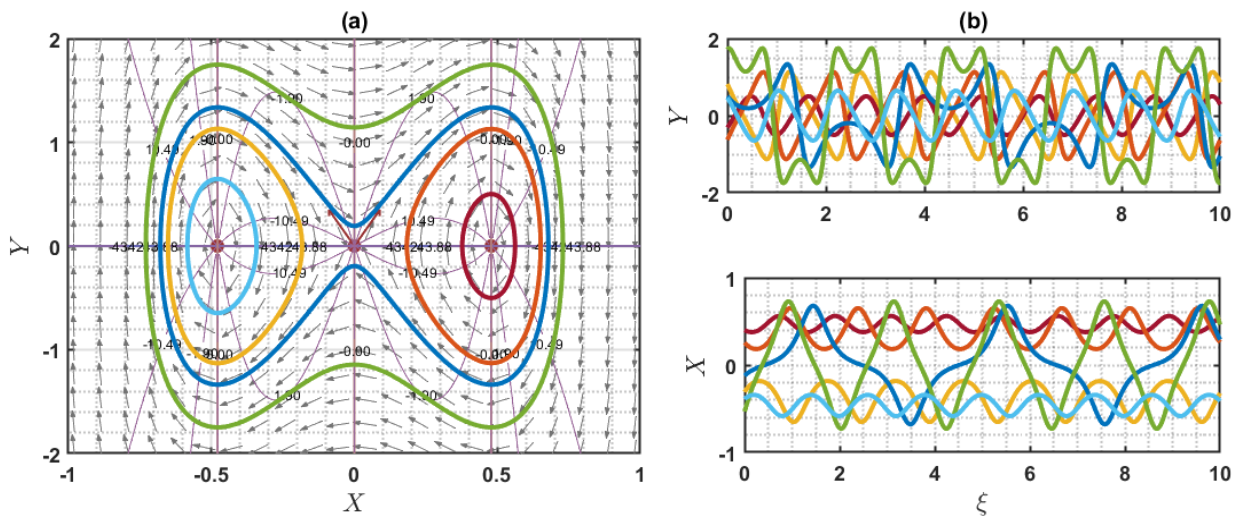


**Figure 8:** The phase depiction and related solution of the planar dynamical system (4.1) are existing for fixed parameter as  $\omega = -0.03, \beta = -12, \tau = -0.21, \alpha = -1.75$ : (a) The possible EP at  $(0,0)$  which is an unstable saddle and the other EP at  $(\pm 0.48, 0)$  are centers, (b) the corresponding solutions of the trajectories in terms of wave variable is depicted.

## 5. Conclusion

In this study, we employed two distinct analytical approaches, namely the AAE and IFE methods, to analyze the (2+1)-dimensional LSWRI equation. Through these methods, we successfully derived a range of solutions, including periodic, kink, exponential, and rational solutions, for this model. The impact of various parameters was also discussed, as illustrated in Figs. 1, 2, 3, and 4. These methods proved effective in achieving the objectives of our scientific investigation. To visually represent different wave patterns under various system parameters, we generated several graphs. These results contribute to a better understanding of the physical implications of the model under scrutiny, as well as other nonlinear models commonly used in research. Additionally, we conducted bifurcation analysis of the model and investigated the phase-chart of the system, as depicted in Figs. 5, 6, 7, and 8. This comprehensive analysis provides valuable insights for future studies on more complex higher-order nonlinear phenomena, along with additional analyses of the model and its soliton solutions.

**Acknowledgements:** The authors would like to thank the editor of the journal and anonymous reviewer for their generous time in providing detailed comments and suggestions that helped us to improve the paper.

**Conflict of interest:** There is no conflict of interest.

**Data availability:** The authors confirm that the data supporting the findings of this study are available within the article.

**Funding:** There is no funding to acknowledge this research.

## References

- [1] K. J. Wang, Resonant Y-type soliton, X-type soliton and some novel hybrid interaction solutions to the (3+1)-dimensional nonlinear evolution equation for shallow-water waves, *Physica Scripta*, 99(2): 025214 (2024).
- [2] S. J. Chen, Y. H. Yin and X. Lü, Elastic collision between one lump wave and multiple stripe



- waves of nonlinear evolution equations, *Communications in Nonlinear Science and Numerical Simulation*, 130; 107205 (2024).
- [3] M. Sadaf, G. Akram and S. Arshed, Optical exact soliton solutions of nonlinear optical transmission equation using two explicit methods, *Optical and Quantum Electronics*, 56(4): 550 (2024).
- [4] M. Iqbal, D. Lu, A. R. Seadawy and Z. Zhang, Nonlinear behavior of dust acoustic periodic soliton structures of nonlinear damped modified Kortewege-de Vries equation in dusty plasma, *Results in Physics*, 59: 107533 (2024).
- [5] S. M. R. Islam, Bifurcation analysis and exact wave solutions of the nano-ionic currents equation: Via two analytical techniques, *Results in Physics*, 58: 107536 (2024).
- [6] C. Yue and C. Shen, Lie Symmetry Analysis for the Fractal Bond-Pricing Model of Mathematical Finance, *Journal of Mathematics*, 2024: 9926131 (2024).
- [7] S. M. R. Islam, S. M. Y. Arafat, H. Alotaibi and M. Inc, Some optical soliton solution with bifurcation analysis of the paraxial nonlinear Schrödinger equation, *Optical and Quantum Electronics*, 56(3): 379 (2024).
- [8] S. M. R. Islam, K. Khan and M. A. Akbar, Optical soliton solutions, bifurcation and stability analysis of the Chen-Lee-Liu model, *Results in Physics*, 57: 106620 (2023).
- [9] K. Kamrujjaman, A. Ahmed and S. Ahmed, Competitive Reaction-diffusion Systems: Travelling Waves and Numerical Solutions, *Advances in Research*, 19(6): 1-12 (2019).
- [10] K. Kamrujjaman, A. Ahmed and J. Alam, Travelling Waves: Interplay of Low to High Reynolds Number and Tan-Cot Function Method to Solve Burger’s Equations, *Journal of Applied Mathematics and Physics*, 7: 861-873 (2019).
- [11] W. Hamali, J. Manafian, M. Lakestani, A. M. Mahnashi and A. Bekir, Optical solitons of M-fractional nonlinear Schrödinger’s complex hyperbolic model by generalized Kudryashov method, *Optical and Quantum Electronics*, 56(1): 7 (2024).
- [12] S. Phoosree, N. Khongnual, J. Sanjun, A. Kammanee and W. Thadee, Riccati sub-equation method for solving fractional flood wave equation and fractional plasma physics equation, *Partial Differential Equations in Applied Mathematics*, 10: 100672 (2024).
- [13] S. M. R. Islam, H. Ahmad, K. Khan, H. F. Wang, M. A. Akbar, F.A. Awwad and E. A. A. Ismail, Stability analysis, phase plane analysis, and isolated soliton solution to the LGH equation in mathematical physics, *Open Physics*, 21(1): 20230104 (2023).
- [13] S. M. R. Islam and K. Khan, Investigating wave solutions and impact of nonlinearity: Comprehensive study of the KP-BBM model with bifurcation analysis, *Plos One*. (In press) 2024. <https://doi.org/10.1371/journal.pone.0300435>
- [15] D. Shi, H. U. Rehman, I. Iqbal, M. Vivas-Cortez, M. S. Saleem and X. Zhang, Analytical study of the dynamics in the double-chain model of DNA, *Results in Physics*, 52: 106787 (2023).
- [16] M. N. Hossain, M. M. Miah, A. H. Ganie, M. S. Osman, and W. X. Ma, Discovering new abundant optical solutions for the resonant nonlinear Schrödinger equation using an analytical technique, *Optical and Quantum Electronics*, 56(5), 847 (2024).
- [17] J. L. Zhang, M. L. Wang, Y. M. Wang and Z. D. Fang, The improved F-expansion method and its applications, *Physics Letter A*, 350(1-2): 103-109 (2006).
- [18] S. M. R. Islam and U. S. Basak, On traveling wave solutions with bifurcation analysis for the nonlinear potential Kadomtsev-Petviashvili and Calogero–Degasperis equations, *Partial Differential Equation and Applied Mathematics*, 8: 100561 (2023).
- [19] S. M. R. Islam, D. Kumar, E. Fendzi-Donfack and M. Inc, Impacts of nonlinearity and wave dispersion parameters on the soliton pulses of the (2+1)-dimensional Kundu-Mukherjee-Naskar equation, *Revista Mexicana Física*, 68(6): 061301 (2022).

- [20] S. Devnath, S. Khan and M. A. Akbar, Exploring solitary wave solutions to the simplified modified camassa-holm equation through a couple sophisticated analytical approaches. *Results in Physics*, 59: 107580 (2024).
- [21] F. Batool, G. Akram, M. Sadaf and U. Mehmood, Dynamics investigation and solitons formation for (2+1)-dimensional zoomeron equation and foam drainage equation, *Journal of Nonlinear Mathematical Physics*, 30(2): 628-645 (2023).
- [22] A. Jhangeer, A. R. Ansari, M. Imran, M. B. Riaz and A. M. Talafha, Application of propagating solitons to Ivancevic option pricing governing model and construction of first integral by Nucci's direct reduction approach, *Ain Shams Engineering Journal*, 15(4): 102615 (2024).
- [23] S. Malik, S. Kumar, A. Akbulut and H. Rezazadeh, Some exact solitons to the (2+1) dimensional Broer-Kaup-Kupershmidt system with two different methods, *Optical and Quantum Electronics*, 55: 1215 (2023).
- [24] M. S. Ahmed, A. A. S. Zaghrouh and H. M. Ahmed, Solitons and other wave solutions for nonlinear Schrödinger equation with Kudryashov generalized nonlinearity using the improved modified extended tanh-function method, *Optical and Quantum Electronics*, 55: 1231(2023).
- [25] S. N. Wang, G. F. Yu and Z. N. Zhu, General soliton and (semi-) rational solutions of a (2+1)-Dimensional Sinh-Gordon equation, *Journal of Nonlinear Mathematical Physics*, 30: 1621-1640 (2023).
- [26] J. X. Niu, R. Guo and J. W. Zhang, Solutions on the periodic background and transition state mechanisms for the higher-order Chen–Lee–Liu equation, *Wave Motion*, 123: 103233 (2023).
- [27] M. J. Ablowitz and P. A. Clarkson, Solitons, nonlinear evolution equations and inverse scattering, Cambridge University press, 149: (1991).
- [28] O. M. Phillips, The dynamics of the upper ocean Cambridge University Press: London. New York, Melbourn, (1977).
- [29] N. Yajima and M. Oikawa, Formation and interaction of sonic-Langmuir solitons: inverse scattering method, *Progress of Theoretical Physics*, 56(6): 1719-1739 (1976).
- [30] Y. C. Ma and L. G. Redekopp, Some solutions pertaining to the resonant interaction of long and short waves, *Physics of Fluids*, 22(10): 1872-1876 (1979).
- [31] R. M. Miura, Backlund transformations, the inverse scattering method, solitons, and their applications: proceedings of the NSF Research Workshop on Contact Transformations, held in Nashville, Tennessee, Springer, 515: 1974.
- [32] D. J. Benney, A general theory for interactions between short and long waves, *Studies in Applied Mathematics*, 56(1): 81-94 (1977).
- [33] R. H. J. Grimshaw, The modulation of an internal gravity-wave packet, and the resonance with the mean motion, *Studies in Applied Mathematics*, 56(3): 241-266 (1977).
- [34] M. Funakoshi and M. Oikawa, The resonant interaction between a long internal gravity wave and a surface gravity wave packet. *Journal of the Physical Society of Japan*, 52(6): 1982-1995 (1983).
- [35] M. Oikawa, M. Okamura and M. Funakoshi, Two-Dimensional Resonant Interaction between Long and Short Waves, *Journal of the physical society of japan*, 58(12): 4416-4430 (1989).
- [36] H. Wen-Hua, Z. Jie-Fang and S. Zheng-Mao, Coherent soliton structures of the (2+1)-dimensional long-wave-short-wave resonance interaction equation, *Chinese Physics*, 11(11): 1101 (2002).
- [37] Z. Yan, Elliptic Function Solutions of (2+ 1)-dimensional Longwave–Shortwave Resonance Interaction Equation via a sinh-Gordon Expansion Method, *Zeitschrift für Naturforschung A*, 59(1-2): 23-28 (2004).
- [38] R. Radha, C. S. Kumar, M. Lakshmanan, X. Y. Tang and S. Y. Lou, Periodic and localized

solutions of the long wave-short wave resonance interaction equation, *Journal of Physics A: Mathematical and General*, 38(44): 9649 (2005).

[39] J. Xin, B. Guo, Y. Han and D. Huang, The global solution of the (2+1)-dimensional long wave-short wave resonance interaction equation, *Journal of Mathematical Physics*, 49: 073504 (2008).

[40] H. Kumar and F. Chand, Exact traveling wave solutions of some nonlinear evolution equations, *Journal of Theoretical and Applied Physics*, 8: 1-10 (2014).

[41] M. Mirzazadeh, Modified simple equation method and its applications to nonlinear partial differential equations. *Information Sciences Letters*, 3(1): 1 (2014).

[42] T. Kanna, M. Vijayajayanthi and M. Lakshmanan, Mixed solitons in a (2+1)-dimensional multicomponent long-wave-short-wave system, *Physical Review E*, 90(4): 042901 (2014).

[43] A. Khare, T. Kanna and K. Tamilselvan, Elliptic waves in two-component long-wave-short-wave resonance interaction system in one and two dimensions, *Physics Letters A*, 378(42): 3093-3101 (2014).

[44] J. Chen, B. F. Feng, Y. Chen and Z. Ma, General bright–dark soliton solution to (2+1)-dimensional multi-component long-wave-short-wave resonance interaction system, *Nonlinear Dynamics*, 88: 1273-1288 (2017).

[45] R. Cimpoiasu and A. S. Pauna, Complementary wave solutions for the long-short wave resonance model via the extended trial equation method and the generalized Kudryashov method, *Open Physics*, 16(1), 419-426 (2018).

[46] H. X. Jia and D. W. Zuo, Interaction of the variable-coefficient long-wave-short-wave resonance interaction equations, *Modern Physics Letters B*, 33(01), 1850426 (2019).

**Appendix**

Consider nonlinear evolution equations in the following structure,

$$N(u, u_t, u_x, u_{xx}, u_{tx}, u_{tt}, \dots) = 0, \tag{A}$$

where  $N$  is a nonlinear polynomial function of wave function  $u(x, t)$ , and including its disparate partial derivatives. We suppose that

$$u(x, y, t) = U(\xi), \xi = x + (\omega - 2\alpha)y + \omega t. \tag{B}$$

In Eq. (B), the coefficients  $\omega$  is the speed of soliton. Eq. (B) converts to Eq. (A) into a nonlinear ordinary differential equation as

$$E(U, U', U'', \dots) = 0, \tag{C}$$

among them, prime represents the derivative of  $\xi$ .

**Appendix A: Advanced Auxiliary equation scheme [13, 14]**

According to the AAE method, the solution of Eq. (C) is conjecture to be

$$U(\xi) = \sum_{i=0}^N c_i d^{if(\xi)}, \tag{A1}$$

where the constants  $c_0, c_1, c_2, \dots, c_N$  are calculated, such that  $c_N \neq 0$ , according to the balanced theorem, we get value  $N$  in Eq. (A1) and  $f(\xi)$  are the solution of the equation as

$$f'(\xi) = \frac{1}{\ln(d)} \{ \lambda d^{-f(\xi)} + \mu + \sigma d^{f(\xi)} \} \tag{A2}$$

In this step, we are substituting the Eq. (A1) and Eq. (A2) into Eq. (C) and we get an algebraic equation which are equated left and right side based on powers of  $d^{if(\xi)}$ , ( $i = 0, 1, 2, 3 \dots$ ). As a result, we gain an algebraic equation, solving these equations and we find out the values of  $c_0, c_1, c_2, \dots, c_N$  and  $\sigma$ . The solutions of Eq. (A2) are obtained as follows:

**Case 1:** When  $\mu^2 - 4\lambda\sigma < 0$  and  $\sigma \neq 0$ ,

$$d^{f(\xi)} = -\frac{\mu}{2\sigma} + \frac{\sqrt{4\lambda\sigma - \mu^2}}{2\sigma} \tan\left(\frac{\sqrt{4\lambda\sigma - \mu^2}}{2}\xi\right)$$

Or

$$d^{f(\xi)} = -\frac{\mu}{2\sigma} - \frac{\sqrt{4\lambda\sigma - \mu^2}}{2\sigma} \cot\left(\frac{\sqrt{4\lambda\sigma - \mu^2}}{2}\xi\right)$$

**Case 2:** When  $\mu^2 - 4\lambda\sigma > 0$  and  $\sigma \neq 0$ ,

$$d^{f(\xi)} = -\frac{\mu}{2\sigma} - \frac{\sqrt{\mu^2 - 4\lambda\sigma}}{2\sigma} \tanh\left(\frac{\sqrt{\mu^2 - 4\lambda\sigma}}{2}\xi\right)$$

Or

$$d^{f(\xi)} = -\frac{\mu}{2\sigma} - \frac{\sqrt{\mu^2 - 4\lambda\sigma}}{2\sigma} \coth\left(\frac{\sqrt{\mu^2 - 4\lambda\sigma}}{2}\xi\right)$$

**Case 3:** When  $\mu^2 + 4\lambda^2 < 0$  and  $\sigma \neq 0$  and  $\sigma = -\lambda$ ,

$$d^{f(\xi)} = \frac{\mu}{2\lambda} - \frac{\sqrt{-\mu^2 - 4\lambda^2}}{2\lambda} \tan\left(\frac{\sqrt{-\mu^2 - 4\lambda^2}}{2}\xi\right)$$

Or

$$d^{f(\xi)} = \frac{\mu}{2\lambda} + \frac{\sqrt{-\mu^2 - 4\lambda^2}}{2\lambda} \cot\left(\frac{\sqrt{-\mu^2 - 4\lambda^2}}{2}\xi\right)$$

**Case 4:** When  $\mu^2 + 4\lambda^2 > 0$  and  $\sigma \neq 0$  and  $\sigma = -\lambda$ ,

$$d^{f(\xi)} = \frac{\mu}{2\lambda} + \frac{\sqrt{\mu^2 + 4\lambda^2}}{2\lambda} \tanh\left(\frac{\sqrt{\mu^2 + 4\lambda^2}}{2}\xi\right)$$

Or

$$d^{f(\xi)} = \frac{\mu}{2\lambda} + \frac{\sqrt{\mu^2 + 4\lambda^2}}{2\lambda} \coth\left(\frac{\sqrt{\mu^2 + 4\lambda^2}}{2}\xi\right)$$

**Case 5:** When  $\mu^2 - 4\lambda^2 < 0$  and  $\sigma = \lambda$ ,

$$d^{f(\xi)} = -\frac{\mu}{2\lambda} + \frac{\sqrt{-\mu^2 + 4\lambda^2}}{2\lambda} \tan\left(\frac{\sqrt{-\mu^2 + 4\lambda^2}}{2}\xi\right)$$

Or

$$d^{f(\xi)} = -\frac{\mu}{2\lambda} - \frac{\sqrt{-\mu^2 + 4\lambda^2}}{2\lambda} \cot\left(\frac{\sqrt{-\mu^2 + 4\lambda^2}}{2}\xi\right)$$

**Case 6:** When  $\mu^2 - 4\lambda^2 > 0$  and  $\sigma = \lambda$ ,

$$d^{f(\xi)} = -\frac{\mu}{2\lambda} - \frac{\sqrt{\mu^2 - 4\lambda^2}}{2\lambda} \tanh\left(\frac{\sqrt{\mu^2 - 4\lambda^2}}{2}\xi\right)$$

Or

$$d^{f(\xi)} = -\frac{\mu}{2\lambda} - \frac{\sqrt{\mu^2 - 4\lambda^2}}{2\lambda} \coth\left(\frac{\sqrt{\mu^2 - 4\lambda^2}}{2}\xi\right)$$

**Case 7:** When  $\mu^2 = 4\lambda\sigma$ ,

$$d^{f(\xi)} = -\frac{2 + \mu\xi}{2\sigma\xi}$$

**Case 8:** When  $\lambda\sigma < 0, \mu = 0$  and  $\sigma \neq 0$ ,



$$d^{f(\xi)} = -\sqrt{\frac{-\lambda}{\sigma}} \tanh(\sqrt{-\sigma\lambda} \xi)$$

Or

$$d^{f(\xi)} = -\sqrt{\frac{-\lambda}{\sigma}} \coth(\sqrt{-\sigma\lambda} \xi)$$

**Case 9:** When  $\mu = 0$  and  $\lambda = -\sigma$ ,

$$d^{f(\xi)} = \frac{1 + e^{(-2\sigma\xi)}}{-1 + e^{(-2\sigma\xi)}}$$

**Case 10:** When  $\lambda = \sigma = 0$ ,

$$d^{f(\xi)} = \cosh(\mu\xi) + \sinh(\mu\xi)$$

**Case 11:** When  $\lambda = \mu = K$ , and  $\sigma = 0$ ,

$$d^{f(\xi)} = e^{K\xi} - 1$$

**Case 12:** When  $\mu = \sigma = K$ , and  $\lambda = 0$ ,

$$d^{f(\xi)} = \frac{e^{K\xi}}{1 - e^{K\xi}}$$

**Case 13:** When  $\mu = \lambda + \sigma$ ,

$$d^{f(\xi)} = -\frac{1 - \lambda e^{(\lambda-\sigma)\xi}}{1 - \sigma e^{(\lambda-\sigma)\xi}}$$

**Case 14:** When  $\mu = -(\lambda + \sigma)$ ,

$$d^{f(\xi)} = \frac{\lambda - e^{(\lambda-\sigma)\xi}}{\sigma - e^{(\lambda-\sigma)\xi}}$$

**Case 15:** When  $\lambda = 0$ ,

$$d^{f(\xi)} = \frac{\mu e^{\mu\xi}}{1 - \sigma e^{\mu\xi}}$$

**Case 16:** When  $\sigma = \mu = \lambda \neq 0$ ,

$$d^{f(\xi)} = \frac{1}{2} \left\{ \sqrt{3} \tan\left(\frac{\sqrt{3}}{2} \lambda \xi\right) - 1 \right\}$$

**Case 17:** When  $\sigma = \mu = 0$ ,

$$d^{f(\xi)} = \lambda \xi$$

**Case 18:** When  $\lambda = \mu = 0$ ,

$$d^{f(\xi)} = \frac{-1}{\sigma \xi}$$

**Case 19:** When  $\sigma = \lambda$  and  $\mu = 0$ ,

$$d^{f(\xi)} = \tan(\lambda \xi)$$

**Case 20:** When  $\sigma = 0$ ,

$$a^{f(\xi)} = e^{\mu\xi} - \frac{m}{n}$$

Substituting the values of the constants  $c_i (i = 0, 1, 2, \dots, N)$ ,  $\lambda$ ,  $\mu$  and  $\sigma$  and the function  $f(\xi)$  into (A1), yield abundant wave solutions to the equation (A).

### Appendix B: Improve F-expansion method [17, 18]

According to the IFE method, the solution of Eq. (C) can be represented in the subsequent form:

$$U(\xi) = \sum_{i=0}^N \alpha_i (m + \varphi(\xi))^i + \sum_{i=1}^N \beta_i (m + \varphi(\xi))^{-i} \tag{B1}$$

Here, it's possible for  $\alpha_{-N}$  or  $\alpha_N$  to equal zero, although both  $\alpha_{-N}$  and  $\alpha_N$  cannot be zero

simultaneously. The constants  $\alpha_i$  ( $i = 0, 1, \dots, N$ ) and  $\beta_i$  ( $i = 1, 2, \dots, N$ ) and  $m$  are to be determined subsequently and  $\varphi(\xi)$  satisfies the ODE in the form:

$$\varphi'(\xi) = \kappa + \varphi^2(\xi), \quad (\text{B2})$$

where the prime stands for derivatives with respect to  $\xi$  and  $\lambda$  is the real parameter. We now present three cases of the general solutions of the Riccati Eq. (B2) as follows:

**Case-I:** when  $\kappa < 0$ , we get following hyperbolic solution

$$\varphi(\xi) = -\sqrt{-\kappa} \tanh(\sqrt{-\kappa} \xi)$$

and

$$\varphi(\xi) = -\sqrt{-\kappa} \coth(\sqrt{-\kappa} \xi)$$

**Case-II:** when  $\kappa > 0$ , we get following trigonometric solution

$$\varphi(\xi) = \sqrt{\kappa} \tan(\sqrt{\kappa} \xi)$$

and

$$\varphi(\xi) = -\sqrt{\kappa} \cot(\sqrt{\kappa} \xi)$$

**Case-III:** when  $\kappa = 0$ , we get following rational solution

$$\varphi(\xi) = -\frac{1}{\xi}$$

The determination of the positive integer  $N$  involves balancing the highest-order linear terms with the highest-order nonlinear terms present in Eq. (C). Subsequently, by substituting Eq. (B1) and (B2) into Eq. (C), we derive polynomials in  $(m + \varphi(\xi))^j$  and  $(m + \varphi(\xi))^{-j}$ , ( $j = 1, 2, 3 \dots, N$ ). Equating the coefficients of these polynomials to zero results in an overdetermined set of algebraic equations for  $\alpha_j$  ( $j = 0, 1, 2, 3, \dots, N$ ),  $\beta_j$  ( $j = 1, 2, 3, \dots, N$ ),  $m$ . Solving these mathematical conditions yields the values of the constants. Substituting these constants along with the solutions of Eq. (B2), we obtain novel and comprehensive soliton solutions for the nonlinear evolution equation Eq. (A).